ResearchGate

See discussions, stats, and author profiles for this publication at: https://www.researchgate.net/publication/272134886

Effects of organic salts on polymer–surfactant interactions: Roles of Bu4NBr and Pr4NBr in PVP–SDS complexation

ARTICLE *in* MACROMOLECULES · SEPTEMBER 2014

Impact Factor: 5.8 · DOI: 10.1021/ma5012232

CITATION
1

READS
9

2 AUTHORS, INCLUDING:

Jia-Hsien Lin
National Cheng Kung University
5 PUBLICATIONS **49** CITATIONS

SEE PROFILE

Available from: Jia-Hsien Lin
Retrieved on: 23 January 2016

Macromolecules

Article

pubs.acs.org/Macromolecules

Effects of Organic Salts on Polymer−Surfactant Interactions: Roles of Bu_4NBr and Pr_4NBr in PVP−SDS Complexation

Jia-Hsien Lin and Sheng-Shu Hou*

Department of Chemical Engineering, National Cheng Kung University, Tainan 70101, Taiwan

Supporting Information

ABSTRACT: Pyrene solubulization and NMR spectroscopy were employed to study the competition between two surfactant aggregation processes in aqueous polymer/organic salt/surfactant systems. Two organic salts used in the study are tetrabutylammonium bromide (Bu_4NBr) and tetrapropylammonium bromide (Pr_4NBr). The anionic surfactant sodium dodecyl sulfate (SDS) is known to have moderate interactions with poly(*N*-vinylpyrrolidone) (PVP), which results in the formation of a PVP−SDS aggregation complex. On the other hand, SDS also can associate with tetraalkylammonium bromides (TAABs) to form mixed micelles by a strong electrostatic attraction. The pyrene solubilization experiments reveal that the dominant aggregation in PVP/TAAB/SDS systems is determined by the [SDS]/[TAAB] ratio, and complexation of PVP with SDS does not occur until the [SDS]/[TAAB] ratio is larger than a specific ratio. For example, when [SDS]/[Bu_4NBr] is less than 1.1, only Bu_4N^+−SDS mixed micelles are formed, and the mixed micelles do not associate with PVP. When [SDS]/[Bu_4NBr] is higher than 1.1, polymer-induced SDS aggregation is detected along with the mixed micellization between SDS and Bu_4NBr. More interestingly, the Bu_4N^+ ions do incorporate with the PVP-bound SDS aggregate to form a PVP−(Bu_4N^+−SDS) complex. By means of 2D NOESY and PFG NMR experiments, both structural and dynamic aspects of the aggregate species formed in the PVP/TAAB/SDS solution were studied. An interaction model was proposed to manifest the role of the two TAAB salts for PVP−SDS complexation in the PVP/TAAB/SDS systems.

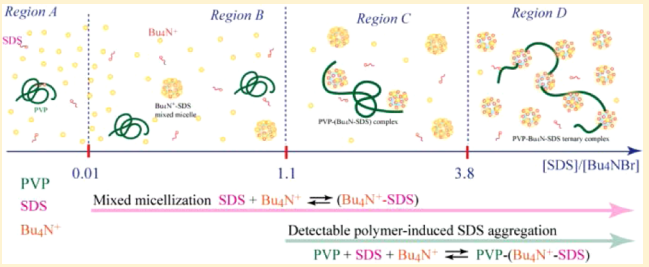

INTRODUCTION

Combinations of polymers and surfactants presents peculiar synergistic behaviors and are of importance in many colloidal applications.[1−3] Many fundamental studies have been directed at understanding the basic mechanisms of polymer−surfactant interactions, especially those focusing on the details of polymer−surfactant interactions at the molecular level.[4−20] One of the features of polymer−surfactant complexation is that the surfactant aggregation appears to begin at a definite surfactant concentration, the critical aggregation concentration (cac), which is smaller than the normal critical micelle concentration (cmc) of the surfactant in the absence of the polymer. In most cases, when the surfactant concentration is higher than the cac, a complex aggregate structure is formed in association with the surfactant molecules and the polymer chain.[21,22] Subsequently, surfactant molecules continue to bind onto the polymer chain until a specific surfactant concentration (P_{sat}) is reached, at which point the polymer chain is saturated with micelle-like surfactant aggregates. The binding ratio of the surfactant to the polymer can thus be calculated from the difference between cac and P_{sat}.

In some situations, salts, including both inorganic and organic ones, are purposefully used together with polymer/surfactant mixtures in technological formulations.[23−25] On the other hand, polymer/surfactant mixtures are usually used in salt environments especially in the cases of biological and pharmaceutical processes.[26,27] A good understanding of the salt effects on polymer−surfactant interactions is thus required for the purpose of tuning the colloidal properties of aqueous solutions containing the polymer, the surfactant and salt. Some recent studies have concentrated on the effects of inorganic salts on polymer−surfactant interactions.[28−39] For neutral polymer/anionic surfactant systems, the externally added salt affects the physicochemical properties of the polymer/surfactant mixture in many ways. Inorganic salts, such as NaCl, normally decrease the surfactant cac, and the cac reduction is enhanced with increases in the salt concentration.[28,32] This is due to a preferential aggregation of surfactant molecules as a result of screening of the repulsive electrostatic repulsions between surfactant headgroups by the excess cations of the added salt. Addition of inorganic salts also promotes the binding affinity and binding ratio of the anionic surfactant to the neutral polymer.[33−35] This has been explained by a "pseudopolycation" model, in which a neutral polymer is coordinated with the cations of the added inorganic salt and thus favorably interacts with the anionic surfactant.[33,40,41] The presence of inorganic salts in polymer/surfactant solutions may lead to decreases in the clouding point (CP) and causes the

Received: June 12, 2014
Revised: August 21, 2014
Published: September 2, 2014

 © 2014 American Chemical Society dx.doi.org/10.1021/ma5012232 | *Macromolecules* 2014, 47, 6418−6429

structural transformation of a polymer−surfactant complex.[36−38] An increase in the salt-induced cloud point (CP) of poly(*N*-vinylpyrrolidone) (PVP) has been observed at high concentrations of sodium dodecyl sulfate (SDS).[39] Moulik et al. suggested that the SDS aggregation on the PVP chain is a dedydration process, in which the number of water molecules on the binding sites of the polymer chain is considerably less than that on the free polymer chain.[39] Moreover, the adjacent surfactant molecules in the PVP−SDS complex are pulled closer by the screening effect arising from salt ions. The structure of the polymer−surfactant complex thus becomes more compact and more insoluable in water, causing the occurrence of phase separation at a lower temperature.

How organic salts influence the complexation between neutral polymers and anionic surfactants still remain mostly unexplored. Nevertheless, some studies[42−44] have reported that the nature of organic counterions significantly affects polymer−surfactant interactions. The counterion effect can be to a certain extent regarded as a sort of salt effect. Zanette et al.[42,43] compared the counterion effects of tetramethylammonium (Me_4N^+) with those of Li^+ or Na^+ on the interaction between poly(ethylene oxide) (PEO) and the dodelcyl sulfate anion (DS^-). They found that the interaction behavior of the PEO/$Me_4N^+DS^-$ system is similar to the classical behavior shown in the PEO/SDS system, even though Me_4N^+ is much more hydrophobic than Na^+. Zana et al.[44] synthesized a homologous series of 1:1 tetraalkylammonium dodecyl sulfates (TAA^+DS^-), which were used for investigation of the counterion effect on the association between DS^- and PVP. Their results indicated that the strength of the polymer−surfactant interaction decreases upon increasing the counterion size. When the alkyl chain length of TAA^+ ion is longer than methyl, no interaction is observed between the polymer and TAA^+DS^-. They also found that although the TAA^+DS^- micelle binds with a large number of hydrophobic TAA^+ ions, the hydrophobic interaction does not help the formation of the polymer-bound surfactant aggregates.

In view of the lack of information on the effects of organic salts on polymer−surfactant interactions, we therefore initiated an extensive investigation of polymer/organic salt/surfactant systems. In this study, the effects of two organic salts, tetraalkylammonium bromides (TAAB), tetrabutylammonium bromide (Bu_4NBr) and tetrapropylammonium bromide (Pr_4NBr), on the complexation behavior of PVP and SDS are examined using fluorescence and NMR techniques. In effect, the hydrophobic Bu_4N^+ ion and Pr_4N^+ ion can bind tightly with SDS to form TAA−SDS mixed micelles.[45] Therefore, in PVP/TAAB/SDS solutions, mixed micellization of TAAB and SDS competes against the establishment of interactions of SDS with PVP, as shown in Scheme 1. The complicated interplay among PVP, TAAB, and SDS results in a novel complexation behavior, which is distinctly different from the three-stage complexation process for the interactions between neutral polymer and anionic surfactant. Contrary to the effect shown by the inorganic salts, Bu_4NBr and Pr_4NBr retard the PVP−SDS interactions; i.e., the SDS cac for the PVP/TAAB/SDS system may be higher than the regular SDS cmc. By varying the [SDS]/[TAAB] ratio, the significant findings in the PVP/TAAB/SDS systems are that the occurrence of PVP−SDS interactions is determined by the [SDS]/[TAAB] ratio and the binding affinity of TAA^+ ions to the surface of SDS aggregates. Complexation of PVP with SDS cannot be detected until the [SDS]/[TAAB] ratio is larger than a specific ratio. The specific ratio is determined by the size of TAA^+ ions, because the SDS aggregation on the polymer chain is resisted by the crowding of the attached TAA^+ ions on the surface of PVP-bound SDS aggregates. Interestingly, we found that the TAA−SDS mixed micelles do not interact with PVP. However, the TAA^+ ions do incorporate with SDS aggregates to form PVP−(TAA−SDS) complexes when PVP starts to interact with SDS. The microstructures of the ternary PVP−(TAA−SDS) complexes were analyzed using two-dimensional nuclear Overhauser effect spectroscopy (2D NOESY) and the pulse-field gradient (PFG) NMR method.

Scheme 1. In the PVP/TAAB/SDS System, Competition of Two Surfactant Aggregation Processes with Each Other[a]

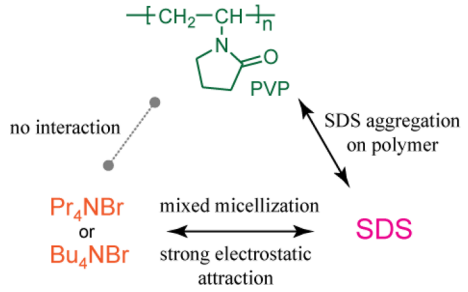

[a]The first type of aggregation is when SDS molecules form PVP−bound aggregates upon interacting with the PVP chain. The second one is when SDS molecules associate with TAA^+ ions to form TAA−SDS mixed micelles as the result of a strong electrostatic attraction.

Although a few studies on the mechanism of how anionic surfactants bind to neutral polymers have been conducted, explanations for the driving forces which induce the biding are not completely satisfactory.[22,32,40,44,46−51] It is generally accepted that the ion−dipole and hydrophobic interactions account for the interactions between neutral polymer and anionic surfactant. In this study, we have shown that, in terms of the structural features of the PVP−(TAA−SDS) complexes, the ion-dipole interaction is the decisive driving force which leads the association of the polymer chain with the surfactant aggregate. We also have demonstrated that the cooperative binding of SDS molecules onto PVP chains is really a dehydration process, which was evidenced by the ^1H chemical shift analysis. Consequently, an effect of dehydration is that some of PVP segments becomes more hydrophobic and thus can penetrate deeply into the core of the PVP-bound SDS aggregate. The hydrophobic interaction further enhances association by the ion-dipole interaction and stabilizes the PVP−SDS complex. These findings advance the current understanding of the binding mechanism for the formation of the polymer-bound surfactant aggregates.

EXPERIMENTAL SECTION

Materials. Sodium dodecyl sulfate (SDS, purity >99%, from J. T. Baker Chemical Co.) and pyrene (from Merck) were recrystallized twice from methanol and then dried in a vacuum oven at 50 °C for 1 week to remove the residual solvent. Ammonium bromide (H_4NBr, purity >99%, from Alfa Aesar), tetrapropylammonium bromide (Pr_4NBr, purity >98%, from Alfa Aesar), and tetrabutylammonium bromide (Bu_4NBr, purity >98%, from Alfa Aesar) were used as received. Poly(*N*-vinylpyrrolidone) (PVP) with $M_w = 4.0 \times 10^4$ g/mol was obtained from Aldrich and used as received.

Pyrene Solubilization and Surface Tension Measurements. A fluorescence spectrophotometer (Hitachi, F2500) was used to measure the pyrene monomer emission spectrum of pyrene-saturated

dx.doi.org/10.1021/ma5012232 | *Macromolecules* 2014, 47, 6418−6429

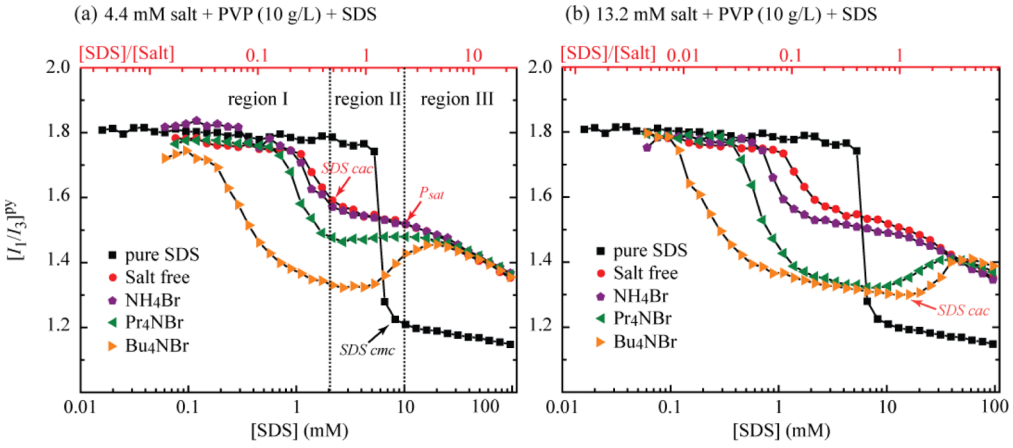

Figure 1. Plots of pyrene I_1/I_3 ratio against log[SDS] for PVP/salt/SDS solutions. The salt concentrations are 4.4 (a) and 13.2 mM (b). In (a), the I_1/I_3–log[SDS] curve (dotted red line) of the binary PVP/SDS system can be divided into three regions (I, II, and III) according to two characteristics, SDS cac and P_{sat}.

PVP/salt/SDS mixed solutions. The slit widths for excitation and emission were 10 and 2.5 nm, respectively. The excitation wavelength was 332 nm and the scan speed was 60 nm/min. The I_1/I_3 ratio was calculated from the intensity of peak I (at 374 nm) and peak III (at 385) in the pyrene fluorescence spectrum. Pyrene-saturated water was prepared by dissolving 3.0 mg of pyrene in 500 mL of deionized water, and the solution was stirred in the dark at ambient temperature for 24 h. Insoluble pyrene was filtered off, and the pyrene concentration was approximately 1.0×10^{-6} M. The PVP/salt/SDS mixed solutions were prepared using pyrene-saturated water. The SDS concentrations were varied from 0.05 to 100 mM. The surface tension of the PVP/salt/SDS mixed solutions was measured with a tensiometer (KRÜSS, K100) using the Wilhelmy plate-detachment method.

NMR Experiments. All NMR experiments were performed at 303.0 K on a Bruker Avance-500 spectrometer equipped with a Bruker 5 mm BBO 500 MHz Z-gradient high-resolution probe at a proton resonance frequency of 500.13 MHz. All NMR data were processed using the software package Bruker Topspin 2.1. The proton chemical shifts were determined relative to an external standard DSS (4,4-dimethyl-4-silapentane-1-sulfonic acid) solution (0.5 wt % in D_2O) in a coaxial tube at 303.0 K, and the chemical shift of DSS was set as δ = 0.00 ppm. The one-dimensional ^{1}H NMR spectra were obtained using the Bruker zg30 pulse program. A total of 128 transients (64k data points) were acquired with a spectral width of 7500 Hz and the 90° pulse was 11.2 μs. The relaxation time was 2 s, and the total acquisition time was about 4.36 s.

The self-diffusion coefficients of the TAA^+ ions, SDS, and PVP were measured by PFG NMR spectroscopy using the Bruker ledbpgp2s pulse program, which is based on the bipolar pulse pair longitudinal-eddy-current delay (BPPLED) pulse sequence.[52] An eddy current delay of 5 ms was incorporated in the pulse sequence to avoid spectral artifacts from the residual eddy current and the delay for gradients recovery (τ) was 0.2 ms. The diffusion time (Δ) was optimized for each sample (50–150 ms). The gradient duration (δ) was kept constant, and the strength of the two pairs of 3.0 ms bipolar square gradients was varied from 2 to 95% in 16 linear increments. The gradient strength was calibrated by measuring the self-diffusion coefficient of the residual HDO signal in a 99.9% D_2O sample (self-diffusion coefficient = 1.902×10^{-9} m^2/s at 25 °C),[53,54] and the maximum gradient strength was found to be 0.562 T/m. The self-diffusion coefficients were calculated using the nonlinear least-squares method based on the following equation:

$$I = I_0 \exp[-D\gamma^2 g^2 \delta^2 (\Delta - \delta/3 - \tau/2)]$$

Here I is the attenuated signal intensity, I_0 is the signal intensity in the absence of the gradient pulse, D is the self-diffusion coefficient, and γ is the magnetiogyric ratio for the proton.

The 2D NOESY spectra were acquired with the standard pulse program (90°–t_1–90°–t_m–90°–acquisition). The NOESY program was run with an 11.2-μs 90° pulse, a 1.5-s relaxation delay, and a 4.7-kHz spectral window. A total of 32 transients were averaged for each of the 256 t_1 increments using time proportional phase incrementation (TPPI) detection. The FID was treated by square-shifted sine bell weighting functions in both dimensions.

RESULTS

PVP–SDS Interactions in PVP/SDS System. The bulk polymer–surfactant interactions were first investigated using pyrene solubilization experiments in order to understand the aggregation process of surfactants and their adsorption onto polymer chains. The intensity ratio of the emission of pyrene at 374 and 385 nm (I_1/I_3) is related to the polarity of surroundings of pyrene. A plot of I_1/I_3 against surfactant concentrations can thus be used to detect the formation of surfactant micelles or polymer-bound surfactant aggregates in the aqueous phase.[12,45,55–57] Additionally, the pyrene I_1/I_3 ratio is a very sensitive polarity index that can be used to recognize which kind of surfactant aggregation is formed in a polymer/surfactant mixed solution.

Figure 1 shows the plots of I_1/I_3 ratios versus log[SDS] (I_1/I_3–log[SDS] curves) for PVP/salt/SDS solutions. The PVP concentration is 10.0 g/L, and the salt concentrations are 4.4 mM (Figure 1a) and 13.2 mM (Figure 1b). In the absence of added salts, the I_1/I_3-log[SDS] curve for the PVP/SDS system (dotted red line) can be divided into three regions (I, II, and III) by two characteristic SDS concentrations, the critical aggregation concentration (cac) and the polymer saturation concentration (P_{sat}). The three different regions correspond to the three stages of the SDS concentration dependence for PVP–SDS interactions.[55] The onset of region II is taken as the SDS cac (ca. 2.0 mM) of the PVP/SDS system at which time SDS molecules start to nucleate on the PVP chain to form micelle-like SDS aggregates. In region II (2 mM < [SDS] < 10 mM), more of the polymer-bound SDS aggregates are formed with increasing [SDS] until the polymer is saturated at [SDS] = ca. 10.0 mM (P_{sat}). The I_1/I_3 value in region II varies slightly from 1.60 to 1.55, indicating that the polarity inside the PVP-bound SDS aggregates is nearly the same. Note that the I_1/I_3 polarity index of 1.60–1.55 can be considered as the characteristic I_1/I_3 value for the PVP-bound SDS aggregate in the absence of added salts. In region III ([SDS] > 10 mM), the

dx.doi.org/10.1021/ma5012232 | Macromolecules 2014, 47, 6418–6429

I_1/I_3 ratio decreases slowly from 1.55 to ca. 1.20, showing that free SDS micelles are formed and coexist with the PVP-bound SDS aggregates.[12]

Effects of TAABs on PVP−SDS Interactions. As seen in Figure 1, the I_1/I_3−log[SDS] curves of the PVP/Pr_4NBr/SDS and PVP/Bu_4NBr/SDS systems are distinctly different from those of the PVP/SDS system and the PVP/NH_4Br/SDS system. This suggests that the added TAABs significantly changes the typical interaction between PVP and SDS, and the effects due to TAABs are obviously unlike those caused by the inorganic salt, NH_4Br. In order to demonstrate the complexity of the associative behaviors among PVP, SDS and TAABs, the I_1/I_3−log[SDS] curve of PVP/Bu_4NBr/SDS ([Bu_4NBr] = 13.2 mM) is replotted in Figure 2 along with the data obtained from

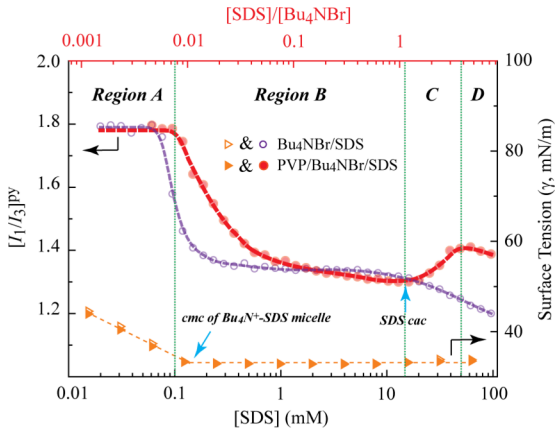

Figure 2. Change in the pyrene I_1/I_3 ratio of the ternary PVP/Bu_4NBr/SDS system ([Bu_4NBr] = 13.2 mM) as a function of [SDS] (broken red line). For comparison, the data obtained from the Bu_4NBr/SDS system[45] in our previous study are plotted as a broken purple line. According to the change in the I_1/I_3 values, the complexation behaviors among PVP, SDS, and Bu_4NBr is divided into four different regions (A−D). Notice that variations in the surface tension with SDS concentration (broken orange lines) for the PVP/Bu_4NBr/SDS and the Bu_4NBr/SDS system are almost the same, providing no information on the complex aggregation among PVP, SDS, and Bu_4NBr.

the Bu_4NBr/SDS system (broken purple line).[45] According to the changes in the I_1/I_3 values, the I_1/I_3−log[SDS] curve of the PVP/Bu_4NBr/SDS (broken red line) is divided into four different regions, which are described in the following paragraphs. The surface tension data of the PVP/Bu_4NBr/SDS and the Bu_4NBr/SDS systems are also given in Figure 2, and it can be seen that the variations in the surface tension with SDS concentration for both systems are almost identical. In addition, only one marked break in the surface tension plot, which corresponds to the cmc of the Bu_4N^+−SDS mixed micelle, is observed. Hence, the surface tension method is unsuitable for investigating ternary PVP/TAAB/SDS systems because it provides no information on the complex aggregation among PVP, SDS, and TAABs.

Region A ([SDS] < ∼ 0.1 mM): the I_1/I_3 value is 1.78, indicating that no distinct hydrophobic microdomains are formed in the solution. Consequently, only free SDS monomers and free Bu_4NBr are present in the solution, and PVP does not interact with either SDS or Bu_4NBr.

Region B (0.1 mM < [SDS] < 14.5 mM and [SDS]/[Bu_4NBr] < 1.1): the I_1/I_3 value first decreases dramatically from 1.78 for [SDS] = 0.1 mM to 1.38 for [SDS] = 0.5 mM and then levels off to a value between 1.38 and 1.26. The first break at [SDS] = 0.1 mM corresponds to the cmc of the Bu_4N^+−SDS mixed micelle. The I_1/I_3 value indicates that the hydrophobic microdomains that form in region B of PVP/Bu_4NBr/SDS system are apparently different from those of the PVP-bound SDS aggregate (I_1/I_3 = 1.60−1.55). With comparison to the Bu_4NBr/SDS system (broken purple line), the polarity of the hydrophobic microdomain formed in region B of the PVP/Bu_4NBr/SDS solution is close to that of the Bu_4N^+−SDS mixed micelle (I_1/I_3 = 1.33).[45] This implies that, in region B, SDS molecules only associate with Bu_4N^+ ions to form Bu_4N^+−SDS mixed micelles even though [SDS] might be much larger than the regular SDS cac (ca. 2.0 mM) for the PVP/SDS system. Additionally, as compared to the Bu_4NBr/SDS system, a more gradual decrease in the I_1/I_3 value is seen for the PVP/Bu_4NBr/SDS system when [SDS] is higher than 0.1 mM. This could be attributed to the fact that the mixed micellization between Bu_4N^+ and SDS is perturbed by the presence of PVP, so the process of forming Bu_4N^+−SDS mixed micelles does not show a sharp cmc.

Region C (14.5 mM < [SDS] < 50 mM and 1.1 < [SDS]/[Bu_4NBr] < 3.8): the I_1/I_3 value shows an unexpected increase from 1.26 for [SDS] = 14.5 mM to 1.40 for [SDS] = 50.0 mM. In principle, if there are two or more different hydrophobic microdomains with different polarities in the aqueous phase, pyrene molecules will be partitioned into these microenvironments.[56,58] The observed I_1/I_3 value should be considered as a weighted average of the polarity in these different hydrophobic microdomains. The gradual increase in the I_1/I_3 value in region C thus means that another less hydrophobic microdomain, as compared to the Bu_4N^+−SDS mixed micelle, is formed when [SDS]/[Bu_4NBr] is larger than 1.1. The less hydrophobic microdomain is the Bu_4N^+−SDS mixed aggregate bound on the PVP chain, which will be confirmed by the NMR experiments in the following sections. It can be concluded that, in region C of the PVP/Bu_4NBr/SDS system, SDS−Bu_4N^+ mixed-micelles coexist with PVP-bound Bu_4N^+−SDS aggregates in the solution. In Figures 1a and 1b, the rise in the I_1/I_3 ratio begins at the same [SDS]/[Bu_4NBr] ratio (ca. 1.1), regardless of the concentration of Bu_4NBr. Consequently, in the presence of Bu_4NBr, the adsorption of SDS molecules onto PVP is directly related to the [SDS]/[Bu_4NBr] ratio.

Region D (50 mM < [SDS] < 100 mM): as can be seen in Figure 2 and Figure 1b, the I_1/I_3 curve for the PVP/Bu_4NBr/SDS system coincides with that of the PVP/SDS system. This suggests that the average polarity of the hydrophobic microdomains in region D of the PVP/Bu_4NBr/SDS system is the same as the average polarity for the free SDS micelles and PVP-bound SDS aggregates in region III of the binary PVP/SDS system. In region D, [SDS]/[Bu_4NBr] is larger than 3.8; the effect of Bu_4NBr is diluted by the large amount of SDS, so the bulk interaction behavior in the ternary PVP/Bu_4NBr/SDS system is identical to that exhibited in the binary PVP/SDS system.

Intermolecular Complexation and Microstructure of Aggregate Species in the PVP/Bu_4NBr/SDS System. Using I_1/I_3 as the hydrophobic index, it is shown that the [SDS]/[Bu_4NBr] ratio determines which kinds of aggregate species might be formed in the PVP/Bu_4NBr/SDS system. In this section, the 2D NOESY experiment combined with the PFG NMR self-diffusion measurement are used to further identify the formation and microstructure of these aggregate species. The 2D NOESY NMR is a useful technique for

dx.doi.org/10.1021/ma5012232 | Macromolecules 2014, 47, 6418−6429

elucidating the microstructure of a polymer−surfactant complex, and it has been applied to investigate polymer penetration into surfactant aggregates in aqueous media.[9−13] The self-diffusion coefficients obtained from the PFG NMR experiment, furthermore, give a clear indication of the binding affinity of TAA^+ ions and SDS to the PVP chain, by which we can infer the compositions of aggregate species formed in the PVP/Bu_4NBr/SDS system. The one-dimensional ^1H spectra and assignments of chemical shifts for PVP, SDS, Bu_4NBr, and Pr_4NBr are shown in Figure 3. Three SDS concentrations

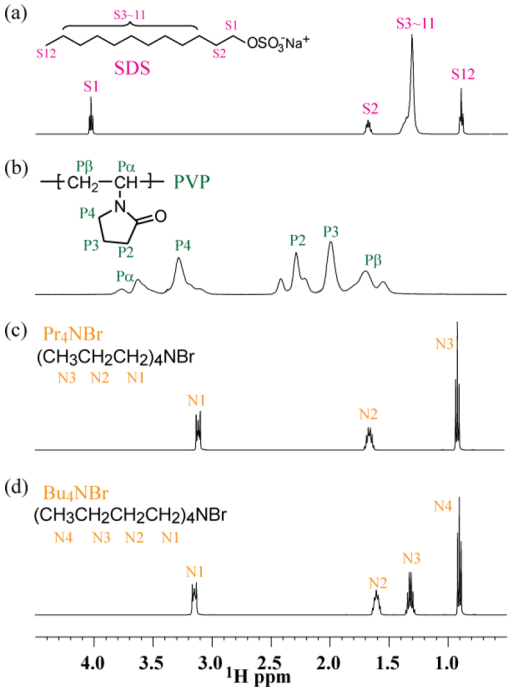

Figure 3. One-dimensional ^1H spectra and assignments of chemical shifts for (a) SDS, (b) PVP, (c) Pr_4NBr, and (d) Bu_4NBr. Notice that the chemical shift of SDS S2 is nearly the same as those of Pr_4NBr N2 and Bu_4NBr N2.

(13.0, 21.6, and 60.0 mM) are selected for the 2D NOESY analysis of the PVP/Bu_4NBr/SDS system (Figure 4) because these concentrations correspond to the end of region B, the start of region C, and region D, as shown in Figure 2.

As shown in Figure 4a ([SDS] = 13.0 mM), the clear cross-peaks between Bu_4N^+ N1 and N2 protons and SDS S3−11protons indicate the formation of the Bu_4N^+−SDS mixed micelle, and the Bu_4N^+ ions are not only attached to the micellar surface but are also inserted into the micellar interior. The signs of intramolecular NOE interactions among the Bu_4N^+ protons are all positive (red contours), but negative NOEs are observed for the S1−S3−11, N1−S3−11, and N2−S3−11 proton pairs. These NOE signs indicate that the molecular tumbling dynamics of the mixed Bu_4N^+−SDS micelle formed in region B is the same as that found in the Bu_4NBr/SDS system.[45]

No cross-peaks are found between the PVP protons and the SDS and Bu_4N^+ protons in Figure 4a, suggesting that the Bu_4N^+−SDS mixed micelle does not bind onto the PVP chain. This could be further verified by the PFG NMR experiment. In the PVP/Bu_4NBr/SDS solution (see Figure 5a), the PVP chain has the slowest translational movement and its self-diffusion coefficient is the smallest ($D_{P,S/Bu} = 0.59 \times 10^{-10}$ m/s^2). If the Bu_4N^+−SDS mixed micelles formed in region B were associated with PVP, the translational motion of SDS and Bu_4N^+ ions would be retarded by the polymer chain. However, the self-diffusion data obtained from the PFG NMR experiment indicate that, when [SDS]/[Bu_4NBr] is less than 1.1, the translational self-diffusion rates of SDS ($D_{S,P/Bu}$) and Bu_4N^+ ($D_{Bu,P/S}$) in the PVP/Bu_4NBr/SDS solution are almost equivalent to those in the Bu_4NBr/SDS system. In addition, the self-diffusion data also show that $D_{P,S/Bu}$ remains constant when [SDS]/[Bu_4NBr] is less than 1.1. It therefore can be concluded that in region B, SDS molecules only aggregate with Bu_4N^+ ions to form Bu_4N^+−SDS mixed micelles, which do not associate with PVP. Figure 5c shows the relative movements of the Bu_4N^+−SDS mixed micelle and the PVP chain in region B. The Bu_4N^+−SDS mixed micelle is not bound to the PVP chain; therefore, the translational movement of the mixed micelle is much faster than the migration rate of the PVP segments.

In Figure 4b ([SDS] = 21.6 mM, region C), the patterns of intramolecular and intermolecular cross-peaks arising from Bu_4N^+ ion and SDS are identical to those shown in Figure 4a, indicating there are also Bu_4N^+−SDS mixed micelles in region C. Furthermore, there are weak cross-peaks (marked by blue rectangle) between the PVP protons (P3 and P4) and the SDS protons (S3−11). It must be emphasized that these PVP−SDS cross-peaks shown in Figure 4b are most likely due to indirect NOE because the NOE build-up is not linear within mixing times smaller than 400 ms (Figure S1, Supporting Information). Therefore, these weak PVP/SDS cross-peaks in Figure 4b result from spin-diffusion among nonadjacent protons that are spaced apart at least 6 Å. A close comparison with the NOESY spectrum of the salt-free PVP−SDS complexes (Figure S2) indicates that the strong PVP/SDS NOE cross-peaks in Figure S2 are really due to primary NOE; in addition, the NOE cross-peaks between the PVP protons and the SDS methyl protons (S12) shown in Figure S2 indicate that the PVP chain penetrates deeply through the PVP-bound SDS aggregate. Thus, for the PVP/Bu_4NBr/SDS system, the lack of direct NOE cross-peaks between PVP and SDS suggests that the PVP segment do not penetrate into the region occupied by the SDS alkyl chains and only thread though the surface of PVP-bound SDS aggregate. In the presence of Bu_4NBr, the NOESY data reveals that the way SDS molecules bind to the PVP chain is apparently different from that in the PVP/SDS system.

In order to more fully understand the microstructure the PVP-bound SDS aggregate formed in region C, a key question needs to be addressed: inasmuch as a very strong electrostatic attraction exists between Bu_4N^+ and SDS, does not Bu_4N^+ associate with PVP by attaching on the surface of the PVP-bound SDS aggregate? That is, in region C, the Bu_4N^+ ions not only aggregate with SDS molecules to form Bu_4N^+−SDS mixed micelles but also attach to SDS aggregates to form a PVP−(Bu_4N^+−SDS) complex. This argument could be answered by the results obtained from the PFG NMR experiment. The self-diffusion data in Figure 5a show that when [SDS]/[Bu_4NBr] is larger than 1.1, the translational movements both for SDS and Bu_4N^+ become slower than those observed in the Bu_4NBr/SDS system. This means that the self-diffusion rates of a certain fraction of SDS and Bu_4N^+ are reduced by the slow moving PVP chains because the observed self-diffusion coefficient is a population-weighted average between fast- and slow-moving species. On the other hand in Figure 5a, it can be seen that when [SDS]/[Bu_4NBr] is greater than 1.1, the translational movement of PVP segments also are hindered by the polymer-

dx.doi.org/10.1021/ma5012232 | Macromolecules 2014, 47, 6418−6429

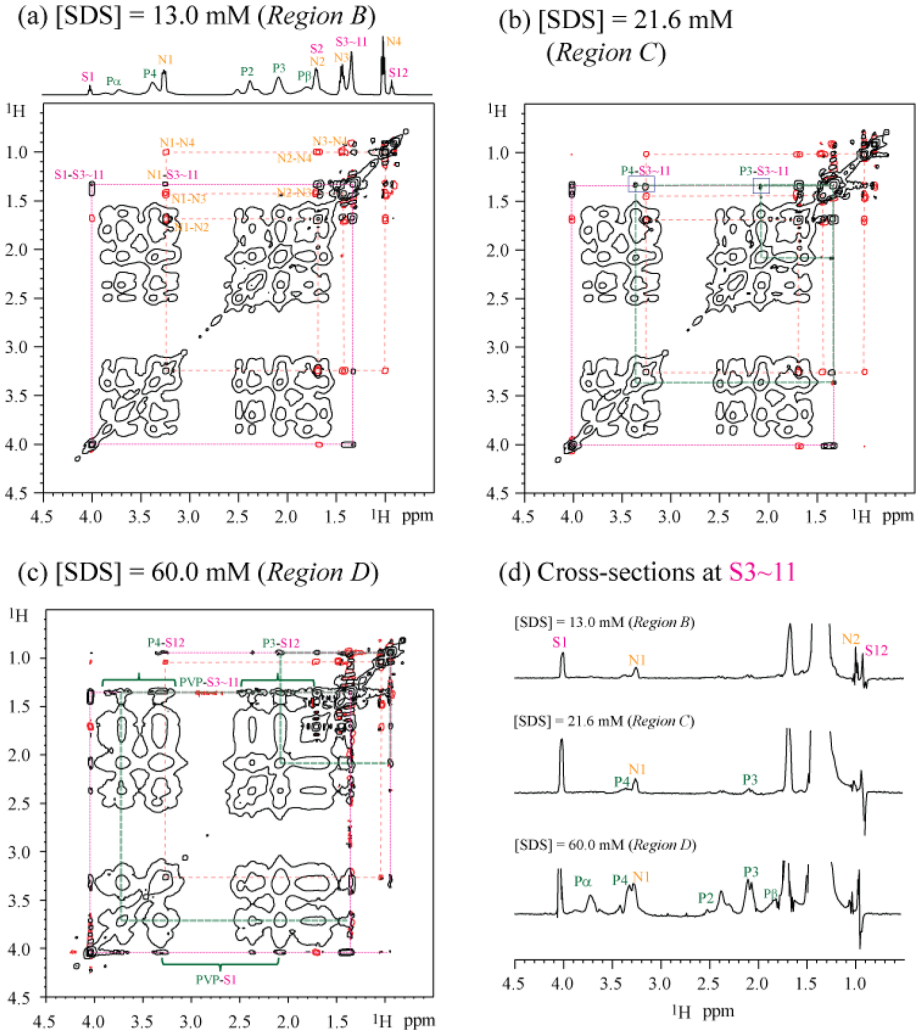

Figure 4. (a–c) 2D ^{1}H–^{1}H two-dimensional NOESY spectra of PVP/Bu_4NBr/SDS solutions obtained with a mixing time of 400 ms. [SDS] = (a) 13.0 mM (region B), (b) 21.6 mM (region C), and (c) 60.0 mM (region D). [PVP] = 10 g/L and [Bu_4NBr] = 13.2 mM. The contour levels in the spectra are linearly spaced. Positive NOE cross-peaks are plotted as red contour lines. (d) Cross sections taken at S3–11 along the ω_2 from each 2D spectrum.

bound Bu_4N^+–SDS aggregates, leading to a slight reduction of $D_{P,S/Bu}$.

It can be concluded that, in region C of the PVP/Bu_4NBr/SDS system, free Bu_4N^+–SDS mixed micelles and PVP-bound Bu_4N^+–SDS aggregates coexist in the solution. Figure 5d depicts the microstructure of the PVP-bound Bu_4N^+–SDS aggregates in region C. It can be seen that the Bu_4N^+–SDS mixed aggregate is partly encompassed by the PVP segments and that its translational diffusion is substantially hampered by the PVP chain. It should be noted that in Figure 4b, no cross-peaks can be observed between PVP and Bu_4NBr, suggesting that the PVP chain is not in proximity to the Bu_4N^+ ions even though the Bu_4N^+ ions are absorbed on the PVP-bound Bu_4N^+–SDS aggregate.

When [SDS] is 60.0 mM in the PVP/Bu_4NBr/SDS system, the NOESY spectrum in Figure 4c shows that all SDS protons have cross-peaks with PVP protons. The NOE build-up (Figure S1) also indicates that the cross-peaks in Figure 4c (mixing time <400 ms) are really due to the primary NOE between PVP and SDS. Specifically, the presence of cross-peaks between PVP and S12 suggests that the PVP chain penetrates through the core of the polymer-bound Bu_4N^+–SDS aggregates. The positive NOE correlation among the protons of the Bu_4N^+ ion in Figure 4c indicates that there must be free Bu_4N^+–SDS mixed micelles in region D. The self-diffusion data in Figure 5a further show that as [SDS] > 60.0 mM, the self-diffusion coefficients of Bu_4N^+ ($D_{Bu,P/S}$) is nearly the same as those of SDS ($D_{S,P/Bu}$), suggesting that almost all of the Bu_4N^+ ions are attached on the PVP-bound SDS aggregates or the free Bu_4N^+–SDS mixed micelles.

PVP/Pr_4NBr/SDS System. In terms of analyses analogous to those that have been done with the PVP/Bu_4NBr/SDS system, the role of Pr_4NBr on PVP–SDS complexation, overall, is similar to that observed for Bu_4NBr in the PVP/Bu_4NBr/SDS system. As shown in Figure 1b (13.2 mM of Pr_4NBr), the I_1/I_3 curve for the PVP/Pr_4NBr/SDS system also can be divided into four regions. The cmc for the Pr_4N^+–SDS mixed-micelle is taken as the first drop in the I_1/I_3 ratio at [SDS] = 0.6 mM. When [SDS] is higher than the cmc, the I_1/I_3 ratio decreases to ca. 1.35, which represents the polarity of the SDS-Pr_4N^+ mixed-micelle.[45] The main difference to be noted is that rises in the I_1/I_3 curve can be found at the [SDS]/[Pr_4NBr] ratio = ca. 0.6 ([Pr_4NBr] = 7.9 mM), which is indicative of the onset of PVP–SDS complexation. In Figure 1a (4.4 mM of

dx.doi.org/10.1021/ma5012232 | Macromolecules 2014, 47, 6418–6429

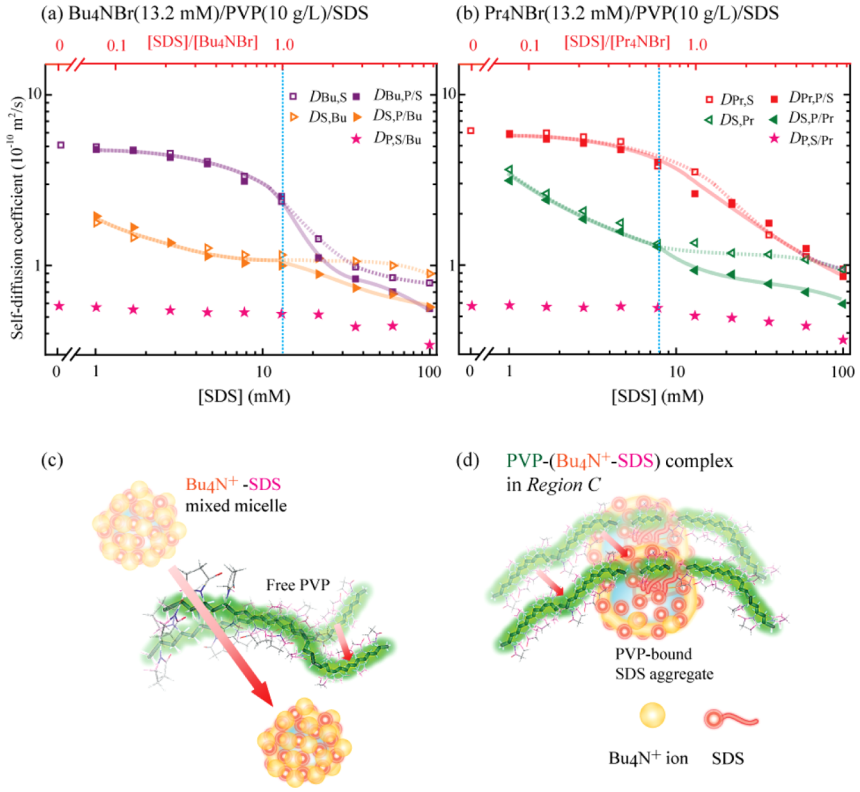

Figure 5. Apparent self-diffusion coefficients of PVP, SDS, and TAA^+ ion as a function of SDS concentration: (a) PVP/Bu_4NBr/SDS and Bu_4NBr/SDS[45] systems, (b) PVP/Pr_4NBr/SDS and Pr_4NBr/SDS[45] systems. $D_{Bu,P/S}$, $D_{S,P/Bu}$, and $D_{P,P/S}$ are the self-diffusion coefficients for Bu_4N^+, SDS, and PVP in the PVP/Bu_4NBr/SDS system. $D_{Bu,S}$ and $D_{S,Bu}$ are the self-diffusion coefficients for Bu_4N^+ and SDS in the Bu_4NBr/SDS system without the added salt. The same notations are used for the PVP/Pr_4NBr/SDS and Pr_4NBr/SDS systems. (c) In region B ([SDS]/[Bu_4NBr] < 1.1), only mixed micellization is observed, and the mixed Bu_4N^+−SDS mixed micelle does not bind to the PVP chain. The translational movement of the mixed micelle (fast) is irrelevant to the PVP chain (slow). (d) In region C ([SDS]/[Bu_4NBr] > 1.1), the Bu_4N^+-attached SDS aggregate that is bound on the PVP chain is formed, and the translational movement of the aggregate is significantly detained by the PVP chain.

Pr_4NBr), it can be seen that the increase in the I_1/I_3 ratio also begins at the [SDS]/[Pr_4NBr] ratio = ca. 0.6, again indicating that the occurrence of PVP−SDS interaction in the presence of TAAB is decided by the stoichiometric ratio between SDS and TAAB. The NOESY spectra in Figure 6 and the self-diffusion data in Figure 5b show that when the [SDS]/[Pr_4NBr] ratio is less than 0.6 (region B), the Pr_4N^+−SDS mixed-micelle is not bound to the PVP chain. Additionally, when the [SDS]/[Pr_4NBr] ratio becomes greater than 0.6 (region C), the PVP−(Pr_4N^+−SDS) complex is present together with the Pr_4N^+−SDS mixed-micelle in the solution. Similar to the microstructure of the PVP−(Bu_4N^+−SDS) complex formed in region C, the PVP chain only locates on the surface of the Pr_4N^+−SDS aggregate and is far apart away from the Pr_4N^+ ion. When the [SDS] is 40.0 mM (region D), the NOESY spectrum (Figure 6c) reveals that the PVP chain penetrates deeply into the core of the PVP-bound Pr_4N^+−SDS aggregate.

DISCUSSION

The experimental data described in the above sections show that in the two PVP/TAAB/SDS systems, mixed micellization proceeds as long as [SDS] is higher than the cmc of the TAA−SDS mixed micelles; however, the occurrence of the PVP-induced SDS aggregation is strongly dependent on the [SDS]/[TAAB] ratio. The general complexation features for the two systems are similar, so the PVP/Bu_4NBr/SDS system again is used as an example in order to demonstrate the [SDS]-dependent aggregation processes taking place in the PVP/TAAB/SDS system, as illustrated in Scheme 2. The onset [SDS] for region C in Scheme 2 can be considered as the SDS cac for both PVP/TAAB/SDS systems. The major difference between the two systems is that the SDS cac for the Bu_4NBr case is 14.5 mM, but the SDS cac for the Pr_4NBr case is 7.9 mM. It is worth noting that the SDS cac of the PVP/TAAB/SDS systems is much higher than the regular SDS cac (ca. 2.0 mM) of the PVP/SDS system.

Only Mixed Micellization Observed in Region B. As shown in Scheme 2, the distinction between region A and region B is based on the cmc of the Bu_4N^+−SDS mixed micelle. In the entire region B, SDS molecules only associate with Bu_4N^+ ions to form Bu_4N^+−SDS mixed micelles. Notice that the Bu_4N^+−SDS mixed micelles formed in region B are not bound with the PVP chain. Although [SDS] in region B may be higher than the regular SDS cac of the PVP/SDS system, no complexation between PVP and SDS is observed in region B. On the basis of the thermodynamic model, the polymer-bound SDS aggregates can form only if the concentration of free SDS monomers ($[SDS]_{free}$) is higher the cac.[47,59] Because the self-diffusion rate of the Bu_4N^+−SDS mixed micelle is not influenced by PVP, $[SDS]_{free}$ in region B can be calculated using the two-site exchange model, the data for which are summarized in Table 1. The details of calculation were given in our previous study.[45] From the self-diffusion data in Table 1, $[SDS]_{free}$ in the entire region B is smaller than 1.0 mM. It is thus reasonable to assume that, in region B, SDS cannot form pure single component aggregates on PVP.

dx.doi.org/10.1021/ma5012232 | Macromolecules 2014, 47, 6418−6429

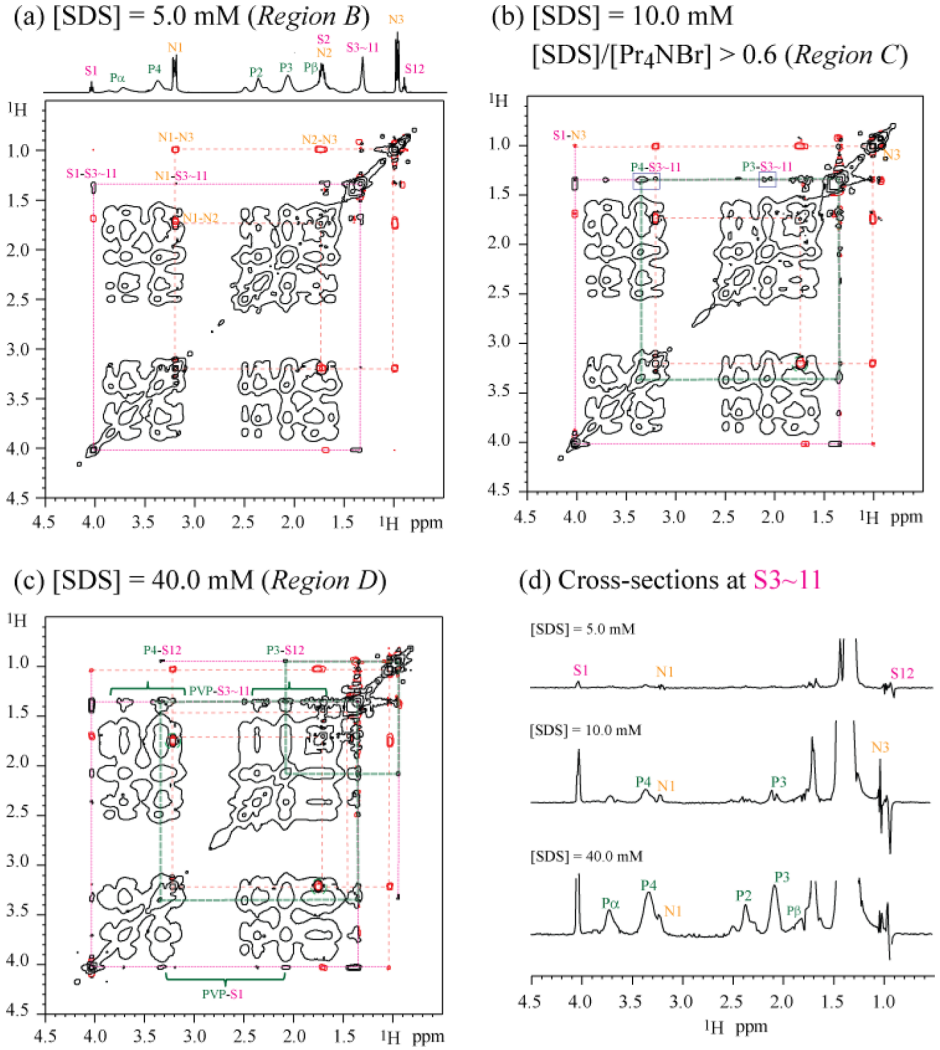

Figure 6. (a–c) 2D ^{1}H–^{1}H two-dimensional NOESY spectra of PVP/Pr_4NBr/SDS solutions obtained with a mixing time of 400 ms. [SDS] = (a) 5.0 mM (region B), (b) 10.0 mM (region C), and (c) 40.0 mM (region D). [PVP] = 10 g/L and [Pr_4NBr] = 13.2 mM. The contour levels in the spectra are linearly spaced. Positive NOE cross-peaks are plotted as red contour lines. (d) Cross sections taken at S3–11 along the ω_2 from each 2D spectrum.

Scheme 2. [SDS]-Dependent Aggregation Processes Taking Place in the PVP/Bu_4NBr/SDS System ([Bu_4NBr] = 13.2 mM)[a]

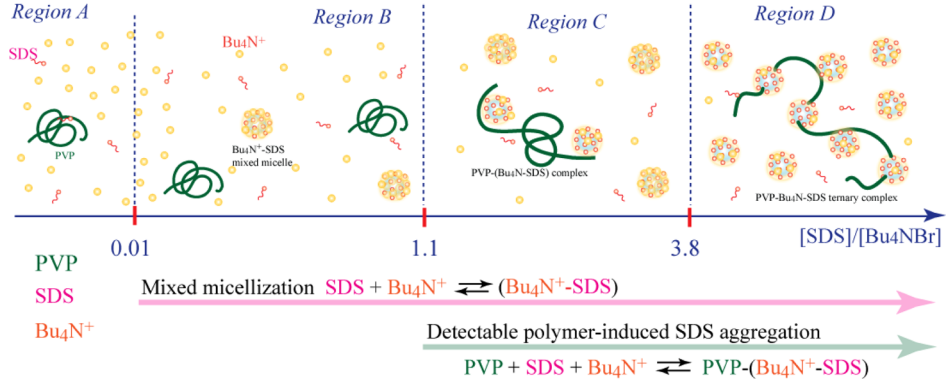

[a]In region B, only mixed micellization between Bu_4NBr and SDS can be observed. In region C, detectable polymer-induced SDS aggregation launches while the mixed micellization is still proceeding. Therefore, the onset [SDS] for region C is considered to be the SDS cac of formation of the PVP–(Bu_4N^+–SDS) complex, in which the PVP segments do not penetrate into the region occupied by the SDS alkyl chains and only thread though the surface of PVP-bound SDS aggregate. In region D, however, microstructure of the PVP–(Bu_4N^+–SDS) complex is similar to that of PVP–SDS complex without the added salt, i.e. the PVP chain penetrates through the core of the polymer-bound Bu_4N^+–SDS aggregates.

dx.doi.org/10.1021/ma5012232 | Macromolecules 2014, 47, 6418–6429

Table 1. Self-Diffusion Coefficients of SDS and TAA^+ in PVP/TAAB/SDS Solutions

composition	[SDS] (mM)	D_{SDS} (10^{-10} m^2/s)[a]	D_{TAA+} (10^{-10} m^2/s)	$[SDS]_{free}$ (mM)[b]	$[TAA^+]_{bound}$ (mM)
PVP/Pr_4NBr/SDS	0	–	11.65	–	–
	1.0	3.13	5.83	0.46	0.74
	1.7	2.41	5.47	0.56	1.58
	2.8	1.86	5.16	0.65	2.31
	4.7	1.57	4.75	0.85	3.28
	7.8	1.28	4.01	1.01	5.04
PVP/Bu_4NBr/SDS	0	–	8.65	–	–
	1.0	1.95	4.79	0.25	0.86
	1.7	1.67	4.71	0.34	1.09
	2.8	1.36	4.30	0.40	2.28
	4.7	1.14	3.95	0.48	3.31
	7.8	1.04	3.12	0.67	5.73
	13.0	1.00	2.54	1.02	7.42

[a] $D_{SDS,free} = 6.13 \times 10^{-10}$ (m^2/s) and $D_{SDS,mic} = 0.56 \times 10^{-10}$ (m^2/s).[45] [b] The concentration of TAABs in the solution was fixed at 13.2 mM.

An interesting finding in this work is that the Bu_4N^+–SDS mixed micelle in region B does not interact with PVP. In our previous study,[45] we demonstrated that the change in the ^1H chemical shift of the α-methylene protons (α-CH_2) next to the SDS sulfate group could be used as an indicator for the degree of hydration on the SDS micellar surface. Dehydration of the SDS headgroup results in an upfield chemical shift of SDS α-CH_2. Figure 7 shows that when the [SDS]/[Br_4NBr] ratio is less than 1.1, the surface of the Bu_4N^+–SDS mixed micelle in the PVP/Bu_4NBr/SDS system (solid orange triangles) is extremely dehydrated as a result of the fact that the micellar surface is almost completely covered by hydrophobic Bu_4N^+ ions. The strong hydrophobic nature of the Bu_4N^+–SDS mixed micelle prohibits its interaction with PVP. Thus, it can be understood that the extremely hydrophobic surface of the Bu_4N^+–SDS mixed micelle precludes the SDS headgroups from developing an overlapped hydration shell, which can mediate the dipole-ion interaction between PVP and SDS. These results support the supposition that the binding of SDS to neutral polymers like PEO and PVP is affected by the nature of the micelle-water surface, as has been previously proposed by Cabane et al.[4] and some other researchers.[16,35,44,60−62] The large size of the Bu_4N^+ ions also hinder the biding of mixed micelles to PVP because, to some extent, Bu_4N^+ ions act as the counterions of a Bu_4N^+–SDS mixed micelle.[44]

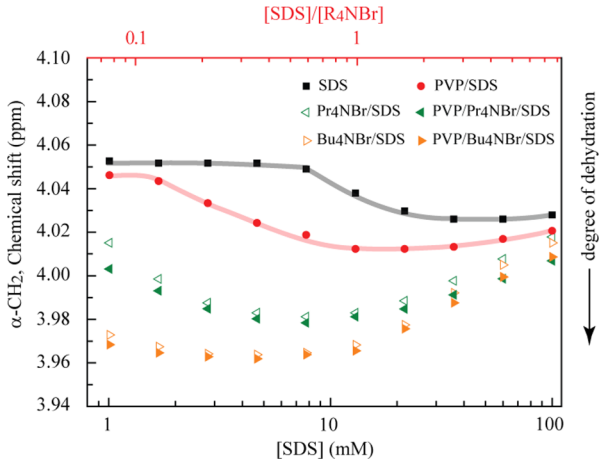

Figure 7. Variation in chemical shifts for α-CH_2 next to the SDS sulfate group as a function of SDS concentration. The upfield shifts of SDS α-CH_2 provide a simple index by which to access the degree of dehydration in the vicinity of the SDS headgroups. The larger the upfield shift, the more dehydrated of the SDS headgroup.

Polymer-Induced SDS Aggregation in Region C. In region C, the binding of the SDS molecules onto the PVP chain is detected while the mixed micellization still in process. The NOESY and PFG NMR experiments further identified that the micelle-like aggregate formed in region C, in fact, is the PVP-bound Bu_4N^+–SDS aggregate, as illustrated in Figure 5d. The important structural features revealed by the NOESY experiments is that the PVP segments are not very close (>6 Å at least) to the SDS alkyl chain and must be positioned far away from the Bu_4N^+ ion. Therefore, the PVP segments only present at the aggregate surface and do not penetrate into the aggregate core. One important issue must be addressed, namely that the PVP segment is located relatively far from the Bu_4N^+ ion in the PVP–(Bu_4N^+–SDS) complex. The PFG NMR data, however, show that the Bu_4N^+ ion do attach on the surface of the PVP-bound SDS aggregate. If the Bu_4N^+ ion was "neutral" to PVP, the PVP segment should have the chance to be in proximity to the Bu_4N^+ ion, thereby giving the NOE correlation or at least leading a magnetization transfer from spin diffusion between them. Therefore, the absence of any correlation in Figure 4b between PVP and the Bu_4N^+ ion means that PVP "dislikes" the Bu_4N^+ ion or, furthermore, that the Bu_4N^+ ion can be regarded as a "polymer-phobic" cation.

In the case of the PVP/SDS system, the PVP chain is found to penetrate deeply into the core of the PVP–SDS aggregate (see Figure S2). This indicates that in addition to the dipole–ion interaction, the hydrophobic interaction between PVP and SDS cannot be ruled out as a driving force that can promote the interaction between PVP and SDS. Similar results have been observed in other neutral polymer/SDS systems.[8−12] In the case of the PVP/Bu_4NBr/SDS system, however, if the hydrophobic interaction between PVP and SDS dominates their complexation, the SDS molecules should be able to bind with the PVP chain via the hydrophobic interaction alone even though the Bu_4N^+ ion might block the dipole-ion interaction between PVP and SDS. The microstructure of the PVP–(Bu_4N^+–SDS) complex in region C obviously shows that the hydrophobic interaction is not the primary reason for establishing the PVP–SDS interaction.

Actually, the cooperative binding of SDS monomers onto PVP chains involves a dehydration process.[16,35,50,60−64] When the SDS molecule approaches the PVP chain, the PVP

dx.doi.org/10.1021/ma5012232 | Macromolecules 2014, 47, 6418−6429

segments replace water molecules in the vicinity of the SDS polar head, and vice versa.[16,35,63] This could be evidenced by the upfield chemical shift of SDS α-CH_2 in the PVP/SDS system (red line in Figure 7). In the case of the PVP/SDS system, when [SDS] is less than P_{sat} (10.0 mM), it can be assumed that there are only PVP-bound SDS aggregates and free SDS monomers in the solution. In Figure 7, at [SDS] = 8.0 mM for the PVP/SDS system, the ^{1}H chemical shift of α-CH_2 of the PVP-bound SDS aggregate is found to be more upfield than that of the pure SDS micelle. Accordingly, the surface of the PVP-bound SDS aggregate is more dehydrated than that of the pure SDS micelle. During the process of SDS adsorption on PVP, some water molecules and counterions (Na^+) are excluded in the space between PVP and SDS. Some of the dehydrated PVP segments thus become hydrophobic enough to interact with the SDS alkyl chain, which bring penetration of the PVP chain into the SDS aggregate core. This hydrophobic interaction between PVP and SDS can further enhance the strength of the PVP−SDS interaction and stabilize the PVP−SDS complex.

Therefore, the dipole−ion interaction is the first and decisive driving force for the PVP−SDS interaction, and the hydrophobic interaction assists in enhancing the PVP−SDS complexation. In region C of the PVP/Bu_4NBr/SDS system, the surface of the PVP-bound SDS aggregate surely is attached with the "polymer-phobic" Bu_4N^+ ion, which blocks the interaction sites between the PVP chain and the SDS headgroups. Moreover, the PVP segments must dodge the surface-attached Bu_4N^+ ion, which significantly weakens the PVP−SDS interaction. As a result, the PVP segments are not dehydrated enough and only can locate at the surface of the SDS aggregate.

Competition between PVP-Induced SDS Aggregation and Mixed Micellization. As mentioned above, the SDS cac of the PVP/Pr_4NBr/SDS system is smaller than that of the PVP/Br_4NBr/SDS system. From Figure 1b, it can be seen that the SDS cac for the PVP/Pr_4NBr/SDS system ([Pr_4NBr] = 13.2 mM) is ca. 7.9 mM, at which the [SDS]/[Pr_4NBr] ratio is about 0.6. In fact, the biding affinity between Pr_4NBr and SDS is almost as strong as that between Br_4NBr and SDS. This can be seen from the fact that $[SDS]_{free}$ at [SDS] = 13.0 mM in the Pr_4NBr/SDS system ([Pr_4NBr] = 13.2 mM) is only 1.8 mM, which is comparable to $[SDS]_{free}$ (1.4 mM) in the Br_4NBr/SDS system ([Bu_4NBr] = 13.2 mM).[45] In addition, the diffusion data in Table 1 show that in the PVP/Pr_4NBr/SDS system, at [SDS] = 7.8 mM, $[SDS]_{free}$ is only 1.0 mM. The above diffusion data indicate that in the PVP/Pr_4NBr/SDS system ([Pr_4NBr] = 13.2 mM), $[SDS]_{free}$ would be smaller than 2.0 mM if only mixed micellization proceeded for [SDS] < 13.2 mM. Logically, the PVP−SDS interaction can only occur when $[SDS]_{free}$ is higher than 2 mM; therefore, the PVP−SDS complexation would not happen under the condition where [SDS] is smaller than [Pr_4NBr], i.e, [SDS] < 13.2 mM in the PVP/Pr_4NBr/SDS system.

The observed PVP−SDS interaction at [SDS]/[Pr_4NBr] = 0.6 in the PVP/Pr_4NBr/SDS system, however, emphatically suggests that the PVP-induced SDS aggregation competes with the mixed micellization between Pr_4NBr and SDS. Namely, in the two PVP/TAAB/SDS systems under investigation, when [SDS] is higher than the regular SDS cac (2.0 mM) but smaller than [TAAB], the PVP-induced SDS aggregation is still likely to occur even though the electrostatic attraction between SDS and TAAB is much stronger than the dipole-ion interaction between PVP and SDS. We thus conclude that in the PVP/TAAB/SDS systems, PVP-induced SDS aggregation proceeds at all times when [SDS] is higher than the normal cac, but the transient PVP-bound SDS aggregate might be very unstable and undetectable at a stage in which [SDS]/[TAAB] is smaller than a specific ratio. This instability of the transient PVP-bound SDS aggregate is explained as follows: As long as PVP-bound SDS aggregate is formed in the PVP/TAAB/SDS solution, the TAA^+ ion must be attached immediately to the SDS aggregate because of the electrostatic attraction. The attached TAA^+ ion obstructs the dipole-ion interaction between PVP and SDS, and the PVP−SDS complex collapses if the SDS aggregate is not large enough to accommodate the "polymer-phobic" TAA^+ ion. The size of the Pr_4N^+ ion is 1.3 times smaller than that of the Br_4N^+ ion. As compared to the case of the Br_4N^+ ion, there will be more space available on the Pr_4N^+-attached surface of the SDS aggregate for close contact of PVP with SDS. In effect, for 1:1 tetraalkylammonium sulfates, the steric hindrance caused by the larger size of the TAA^+ ion decreases the micelle aggregation number and restricts the growth of the micelle.[65] The same inference could be applied to the polymer-induced SDS aggregation with TAA^+ ions: the SDS-bound TAA^+ ions on the aggregate surface can impede further addition of SDS molecules to the PVP-bound SDS aggregate. The less dehydrated micelle surface and aggregate surface for the case of Pr_4NBr shown in Figure 6 also reflect the fact that smaller and less hydrophobic Pr_4N^+ ions result in a more incomplete coverage of these surfaces. Clearly, the binding of SDS molecules onto the PVP chain is easier for the case of Pr_4N^+ than for Bu_4N^+. Therefore, significant PVP−SDS complexation can be observed at [SDS]/[Pr_4NBr] = 0.6 ([SDS] = 7.9 mM).

The Effect of TAAB is Diluted in Region D. As shown in Figures 1 and 2, the beginning of region D is defined as the SDS concentration, at which the I_1/I_3 curves of the two PVP/TAAB/SDS systems are superimposed with that of the PVP/SDS system. In region D, the free TAA−SDS mixed micelles coexist with the PVP−(TAA−SDS) complexes, and the average polarity in these hydrophobic microdomains is identical to that in the free SDS micelles and PVP-bound SDS aggregates in the case of the PVP/SDS system. This means that the effects of TAA^+ ions on the association between PVP and SDS are diluted by the large amount of SDS ions and can thus be ignored. The NOESY spectra in Figures 3d and 5d show that the PVP chains penetrate into the Bu_4N^+-attached SDS aggregate formed in region D, so the microstructure of the PVP−(Bu_4N^+−SDS) complex is very similar to that of PVP−SDS complex without the added salt. On the whole, in region D, the surface-attached TAA^+ ions do not affect the inner structure of the aggregate species and the way in which the SDS molecules bind onto the PVP chain.

CONCLUSIONS

In terms of results obtained from pyrene solubilization, the 2D NOESY, and the PFG NMR experiments, we verified the roles of Bu_4NBr and Pr_4NBr in the complexation between PVP and SDS. Both the Bu_4N^+ ion and the Pr_4N^+ ion are "polymer-phobic" cations that retard PVP−SDS interaction. In the PVP/TAAB/SDS system, as long as [SDS] is higher than the normal cac (ca. 2.0 mM) the PVP-induced SDS aggregation can compete with the mixed micellization between SDS and TAAB. However, at an [SDS]/[TAAB] ratio smaller than a specific value, the TAA^+-attached PVP−SDS complex is very unstable and cannot be detected using the pyrene-solubilization, PFG NMR, and NOESY methods. The specific value is correlated

dx.doi.org/10.1021/ma5012232 | Macromolecules 2014, 47, 6418−6429

with the size and hydrophobicity of the TAA^+ ions and is also dependent on the [TAAB] in the solution. In the presence of TAAB (13.2 mM), significant PVP−SDS complexation can only be observed when [SDS]/[Bu_4NBr] is greater than 1.1 or when [SDS]/[Pr_4NBr] is greater than 0.6. The microstructure of the PVP−(TAA^+−SDS) complex formed in region C is apparently different from that of the PVP−SDS complex without the added salt. In region C, the PVP chain in the PVP−(TAA^+−SDS) complex is located only on the aggregate surface and must be far away from the surface-attached TAA^+ ions. These distinctive structural features explain that the dipole-ion interaction, rather than the hydrophobic interaction, is the primary driving force which dominates the occurrence of PVP−SDS interactions. In summary, the addition of hydrophobic TAAB into a PVP/SDS solution provides a simple route for tuning the occurrence of polymer−surfactant interactions. Furthermore, the unique feature of the microstructure of the PVP−(TAA^+−SDS) complex has the potential to tailor suitable carrier solubilization in the aqueous phases.

■ ASSOCIATED CONTENT

Ⓢ Supporting Information

Buildup curves for the cross-peak volume of the P3−S3−11 pair in the 2D NOESY spectrum (Figure S1) and $^1H-^1H$ two-dimensional NOESY spectrum of the PVP(10 g/L)/SDS(10 mM)/D_2O solution and the microstructure of the PVP−SDS complex (Figure S2). This material is available free of charge via the Internet at http://pubs.acs.org/.

■ AUTHOR INFORMATION

Corresponding Author

*(S.-S.H.) E-mail: Telephone: +886-6-2757575 ext 62641. Fax: +886-6-2344496. E-mail: sshou@mail.ncku.edu.tw..

Notes

The authors declare no competing financial interest.

■ ACKNOWLEDGMENTS

This work was financially supported by a three-year research grant (NSC-99-2628-E-006-002) from *National Science Council* (NSC) of Taiwan. We thank Ms. Ru-Rong Wu for her help in performing the NMR experiments.

■ REFERENCES

(1) Holmberg, K.; Jönsson, B.; Kronberg, B.; Lindman, B. *Surfactants and Polymers in Aqueous Solution*; John Wiley & Sons, Ltd.: Chichester, U.K., 2003.
(2) Tadros, T. F. *Applied Surfactant: Principle and Applications*; Wiley-VCH: Weinheim, Germany, 2005.
(3) Nystroem, B.; Walderhaug, H.; Hansen, F. K.; Lindman, B. *Langmuir* **1995**, *11*, 750−757.
(4) Cabane, B. *J. Phys. Chem.* **1977**, *81*, 1639−1645.
(5) Cabane, B.; Duplessix, R. *J. Phys. (Paris)* **1982**, *43*, 1529−1542.
(6) Goddard, E. D.; Ananthapadmanabhan, K. P. *Interactions of Surfactants with Polymers and Proteins*; CRC Press: Boca Raton, FL, 1993.
(7) Kwak, J. C. T., Ed. *Polymer-Surfactant Systems*; Marcel Dekker: New York, 1998; Vol. 77.
(8) Gao, Z. S.; Wasylishen, R. E.; Kwak, J. C. T. *J. Phys. Chem.* **1991**, *95*, 462−467.
(9) Landry, J. M.; Marangoni, D. G.; Arden, D. A.; MacLennan, I. J.; Kwak, J. C. T. *J. Surf. Deterg.* **2009**, *12*, 155−164.
(10) Roscigno, P.; Asaro, F.; Pellizer, G.; Ortona, O.; Paduano, L. *Langmuir* **2003**, *19*, 9638−9644.
(11) Gjerde, M.; Nerdal, W.; Holand, H. *J. Colloid Interface Sci.* **1996**, *183*, 285−288.
(12) Tzeng, J.-K.; Hou, S.-S. *Macromolecules* **2008**, *41*, 1281−1288.
(13) Hou, S.-S.; Tzeng, J.-K.; Chuang, M.-H. *Soft Matter* **2010**, *6*, 409−415.
(14) Chen, J. Q.; Gong, X. L.; Yang, H.; Yao, Y. F.; Xu, M.; Chen, Q.; Cheng, R. S. *Macromolecules* **2011**, *44*, 6227−6231.
(15) Chen, J. Q.; Xue, H. J.; Yao, Y. F.; Yang, H.; Li, A. M.; Xu, M.; Chen, Q.; Cheng, R. S. E. *Macromolecules* **2012**, *45*, 5524−5529.
(16) Purcell, I. P.; Lu, J. R.; Thomas, R. K.; Howe, A. M.; Penfold, J. *Langmuir* **1998**, *14*, 1637−1645.
(17) Jean, B.; Lee, L.-T.; Cabane, B. *Langmuir* **1999**, *15*, 7585−7590.
(18) Cooke, D. J.; Blondel, J. A. K.; Lu, J.; Thomas, R. K.; Wang, Y.; Han, B.; Yan, H.; Penfold, J. *Langmuir* **1998**, *14*, 1990−1995.
(19) Cooke, D. J.; Dong, C. C.; Lu, J. R.; Thomas, R. K.; Simister, E. A.; Penfold, J. *J. Phys. Chem. B* **1998**, *102*, 4912−4917.
(20) Mears, S. J.; Deng, Y.; Cosgrove, T.; Pelton, R. *Langmuir* **1997**, *13*, 1901−1906.
(21) Goddard, E. D. *Colloids Surf.* **1986**, *19*, 255−300.
(22) Tam, K. C.; Wyn-Jones, E. *Chem. Soc. Rev.* **2006**, *35*, 693−709.
(23) Astruc, D.; Lu, F.; Aranzaes, J. R. *Angew. Chem., Int. Ed.* **2005**, *44*, 7852−7872.
(24) Gouveia, L.; Paillet, S.; Khoukh, A.; Grassl, B.; Müller, A. *Colloids Surf., A* **2008**, *322*, 21−218.
(25) Nystroem, B.; Kjoniksen, A.-L.; Lindman, B. *Langmuir* **1996**, *12*, 3233−3240.
(26) Qi, S.; Roser, S.; Edler, K. J.; Pigliacelli, C.; Rogerson, M.; Weuts, I.; Van Dycke, F.; Stokbroekx, S. *Pharm. Res.* **2013**, *30*, 290−302.
(27) Torchilin, V. P. *Pharm. Res.* **2007**, *24*, 1−16.
(28) Murata, M.; Arai, H. *J. Colloid Interface Sci.* **1973**, *44*, 475−480.
(29) Shirahama, K.; Ide, N. *J. Colloid Interface Sci.* **1976**, *54*, 450−452.
(30) Evertsson, H.; Holmberg, K. *Colloid Polym. Sci.* **1997**, *275*, 830−840.
(31) Majhi, P. R.; Moulik, S. P.; Burke, S. E.; Rodgers, M.; Palepu, R. *J. Colloid Interface Sci.* **2001**, *235*, 227−234.
(32) Minatti, E.; Zanette, D. *J. Colloid Interface Sci.* **1996**, *113*, 237−246.
(33) Norwood, D. P.; Minatti, E.; Reed, W. F. *Macromolecules* **1998**, *31*, 2957−2965.
(34) Sorci, G. A.; Reed, W. F. *Langmuir* **2002**, *18*, 353−364.
(35) Lissi, E. A.; Abuin, E. *J. Colloid Interface Sci.* **1985**, *105*, 1−6.
(36) Holmberg, C. *Colloid Polym. Sci.* **1996**, *274*, 836−847.
(37) Carlsson, A.; Karlström, G.; Lindman, B. *Langmuir* **1986**, *2*, 536−537.
(38) Karlström, G.; Carlsson, A.; Lindman, B. *J. Phys. Chem.* **1990**, *94*, 5005−5015.
(39) Dan, A.; Ghosh, S.; Moulik, S. P. *J. Phys. Chem. B* **2008**, *112*, 3617−3624.
(40) Dubin, P. L.; Gruber, J. H.; Xia, J.; Zhang, H. *Colloid Polym. Sci.* **1992**, *148*, 35−41.
(41) Xia, J.; Dubin, P. L. *J. Phys. Chem.* **1992**, *96*, 6805−6811.
(42) Froehner, S. J.; Belarmino, A.; Zanette, D. *Colloids Surf., A* **1998**, *137*, 131−139.
(43) Zanette, D.; Lima, C. F.; Ruzza, A. A.; Belarmino, A. T. N.; Santos, S. F.; Frescura, V. L. A.; Marconi, D. M. O.; Froehner, S. J. *Colloids Surf., A* **1999**, *147*, 89−105.
(44) Benrraou, M.; Bales, B.; Zana, R. *J. Colloid Interface Sci.* **2003**, *267*, 519−523.
(45) Lin, J.-H.; Chen, W.-S.; Hou, S.-S. *J. Phys. Chem. B* **2013**, *117*, 12076−12085.
(46) Ruckenstein, E.; Huber, G.; Hoffman. *Langmuir* **1987**, *3*, 382−387.
(47) Nikas, Y. J.; Blankstein, D. *Langmuir* **1994**, *10*, 3512−3528.
(48) Wang, G.; Olofsson, G. *J. Phys. Chem. B* **1998**, *102*, 9276−9283.
(49) Li, Y.; Bloor, D. M.; Penfold, J.; Holzwarth, J. F.; Wyn-Jones, E. *Langmuir* **2000**, *16*, 8677−8648.
(50) Griffiths, P. C.; Hirst, N.; Paul, A.; King, S. M.; Heenan, R. K.; Farley, R. *Langmuir* **2004**, *20*, 6904−6913.

(51) Mangiapia, G.; Berti, D.; Baglioni, P.; Teixeira, J.; Paduano, L. *J. Phys. Chem. B* **2004**, *108*, 9772−9779.
(52) Wu, D.; Chen, A.; Johnson, C. S., Jr. *J. Magn. Reson.* **1995**, *115*, 260−264.
(53) Mills, R. *J. Phys. Chem.* **1973**, *77*, 685−688.
(54) Holz, M.; Weingartner, H. *J. Magn. Reson.* **1991**, *92*, 115−125.
(55) Turro, N. J.; Baretz, B. H.; Kuo, P. L. *Macromolecules* **1984**, *17*, 1321−1324.
(56) Kuo, P. L.; Hou, S. S.; Teng, C. K.; Liang, W. J. *Colloid Polym. Sci.* **2001**, *279*, 286−291.
(57) Winnik, F. M.; Regismond, S. T. A. *Colloids Surf., A* **1996**, *118*, 1−39.
(58) Shannigrahi, M.; Bagchi, S. *J. Phys. Chem. B* **2005**, *109*, 14567−14572.
(59) Nagarajan, R. *Colloids Surf.* **1985**, *13*, 1−17.
(60) Kjellander, R.; Florin, E. *J. Chem. Soc., Faraday Trans. 1* **1981**, *77*, 2053−2077.
(61) Witte, F. M.; Engberts, J. B. F. N. *Colloids Surf.* **1989**, *36*, 417−426.
(62) Brackman, J. C.; Engberts, J. B. F. N. *Chem. Soc. Rev.* **1993**, *22*, 85−92.
(63) Chari, K.; Lenhart, W. C. *J. Colloid Interface Sci.* **1990**, *137*, 204−216.
(64) Bloor, D. M.; Holzwarth, J. F.; Wyn-Jones, E. *Langmuir* **1995**, *11*, 2312−2313.
(65) Benrraou, M.; Bales, B. L.; Zana, R. *J. Phys. Chem. B* **2003**, *107*, 13432−13440.